VAK 2024 MODERN ASTRONOMY: FROM THE EARLY UNIVERSE TO EXOPLANETS AND BLACK HOLES
300 years Russian Academy of Sciences

First results of HI survey of recently discovered close dwarf galaxies

A. Nazarova[1], J. Cannon[2], I. Karachentsev[1], D. Makarov[1], and M. Chazov[1]

[1] Special Astrophysical Observatory of the Russian Academy of Sciences, Nizhny Arkhyz, 369167 Russia
[2] Department Physics and Astronomy, Macalester College, 1600 Grand Avenue, Saint Paul, MN 55105 USA

Abstract. We describe the results of observations with the 100m Robert C. Byrd Green Bank Telescope (GBT) in the HI line of 54 nearby dwarf galaxies found mainly in the DESI Legacy Imaging Surveys. Of these, we detected 35 galaxies with the following median parameters: the HI-flux of 0.53 Jy km/s, heliocentric velocity of 1123 km/s, and W_{50} line width of 33 km/s. Most of them are isolated irregular objects, and some have turned out to be new probable satellites of nearby disc galaxies: NGC 2787, NGC 3556, NGC 4490, and NGC 5055. The detected galaxies are predominantly gas-rich systems with a median gaseous-mass-to-stellar-mass ratio of 2.41.

Keywords: galaxies: dwarf; galaxies

DOI: 10.26119/VAK2024.036

1 Introduction

Most existing galaxy catalogues are samples limited by an apparent magnitude or flux of objects in a fixed spectral range. However, the results of modeling the large-scale structure of the Universe within the framework of the standard cosmological model ΛCDM need to be compared with an ensemble of galaxies limited to a fixed volume. The most suitable sample of this type is the Updated Nearby Galaxy Catalog (UNGC, Karachentsev et al. 2013), whose regularly updated database (https://www.sao.ru/lv/lvgdb/) contains about 1400 galaxies with distances $D < 11$ Mpc. It is obvious that the population of this Local Volume (LV) can either increase with the advent of deeper sky surveys, or decrease somewhat as the distances of the galaxies are refined. A great advantage of the UNGC catalog is the predominance of low-luminosity dwarf galaxies, which are usually inaccessible to observations at large distances.

The search for new LV objects (Karachentsev & Kaisina 2022; Karachentseva et al. 2023; Karachentsev et al. 2024) using the DESI Legacy Imaging Surveys (Dey et al. 2019) led to the discovery of more than a hundred high declination dwarf galaxies. About half of them turned out to be spheroidal systems (dSph) with a low neutral hydrogen content. After excluding dSphs, we selected 54 dwarf galaxies with evidence of active star formation to measure their radial velocities with the Green Bank Telescope (GBT).

2 GBT observations of the nearby dwarfs

We observed 54 dwarf galaxies with the National Radio Astronomy Observatory 100m Robert C. Byrd Green Bank Telescope (GBT). The total effective frequency coverage was from 1406 MHz to 1426 MHz. This covers the approximate velocity range of -1000 to $+3000$ km/s, which is sufficient to probe the LV within 10 Mpc. Data were acquired during 14 observing sessions in August and October 2023 ($\sim$ 50 hours in total).

The HI signal was detected in 35 galaxies out of 54 targets. Examples of images from the DESI Legacy Imaging Surveys along with their spectra near the HI line are shown in Fig. 1.

All data reduction was carried out in the IDL environment[1] using the GBTIDL package developed at NRAO. For most galaxies, the velocity and width measurements and their errors were obtained by fitting a single Gaussian component to the line profile after continuum fitting and subtraction. The HI-line total flux was calculated as the area under the real spectrum in a selected region.

[1] Exelis Visual Information Solutions, Boulder, CO.

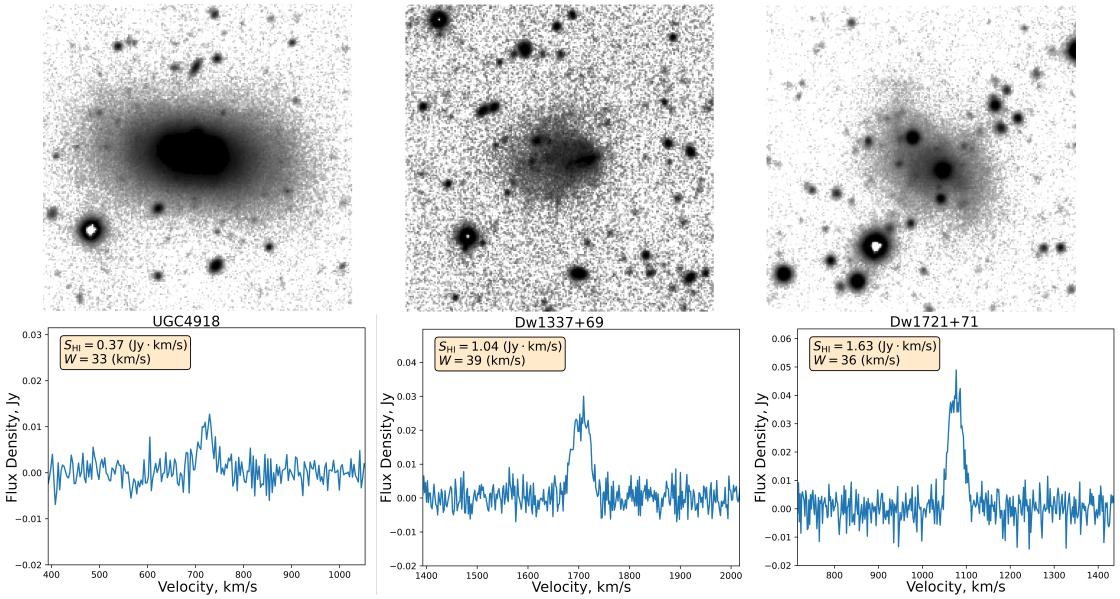

Fig. 1. *Top row.* Images of nearby late-type dwarf galaxies taken from the DESI Legacy Imaging Surveys. Each image side is 2′, North at the top and East at the left. *Bottom row.* HI spectra of these dwarf galaxies detected with the GBT. The total HI-flux $S_{\rm HI}$ and the line width W_{50} are given in each panel.

3 Photometry

Deep multicolour photometry was performed for 52 of the 54 galaxies, using images from the DESI Legacy Imaging Surveys (DR10). The total g, r magnitudes were measured for all 52 objects, z values only for the brightest objects, and i values only when the corresponding images were available. Two targets (Dw1351+50 and Dw1354+44) turned out to be false, non-existent objects.

We measured photometric growth curves using standard ellipse-fitting and aperture photometry techniques in the Astropy *photutils*[2]) package. This was preceded by background subtraction. Foreground and bright background objects were also masked, and the corresponding pixels were then replaced by the mean flux in the elliptical annulus contained in the mask. The resulting growth curve was fitted using a slightly modified exponential law. Some photometric steps are shown in Fig. 2.

4 Discussion

The combination of GBT-observations and optical photometry has been used to estimate the masses of hydrogen $M_{\rm HI}$, neutral gas $M_{\rm gas}$, and the stellar population

[2] https://photutils.readthedocs.io/en/stable/

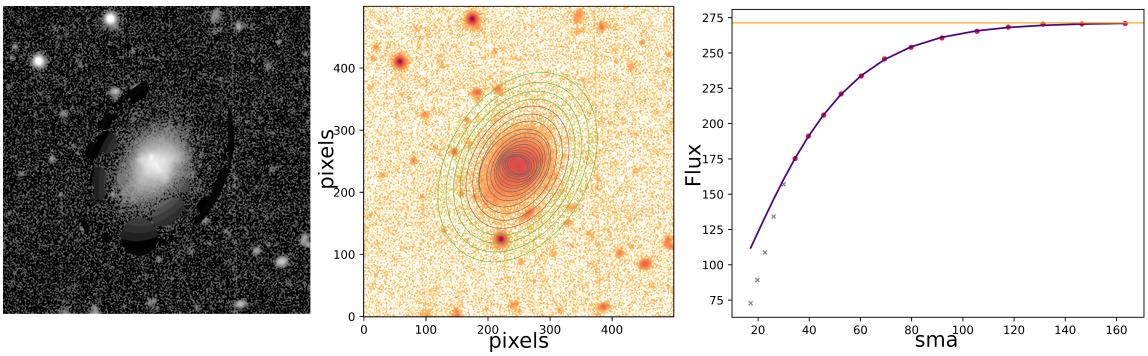

Fig. 2. *Left.* Image of the Dw1558+67 with masked pixels replaced by the mean flux in the aperture rings. *Middle.* Elliptical isophotes fitted to the galaxy image. *Right.* Corresponding growth curve fitted with a modified exponential low.

M_*. It turns out that the mass equality of gas and stars $M_{\rm gas} = M_*$ occurs when $m_{21} = B + 1.00 \pm 0.11$ mag, where $m_{21} = 17.4 - 2.5\log(S_{\rm HI})$, $S_{\rm HI}$ — HI-flux. Consequently, in the late-type dwarf galaxies with $m_{21} - B < 1^m.00$, the gas component predominates.

The distribution of galaxies in our sample according to m_{21} and B magnitudes is shown in the left panel of Fig. 3. Galaxies not detected in the HI line are indicated by open dots with $m_{21} = 20.0$. The diagonal lines correspond to the values of the parameter $\mu = M_{\rm gas}/M_*$ equal to 0.1, 1.0 and 10. The majority of the detected galaxies are gas-dominated systems with a median ratio of $\mu = 2.41$.

The m_{21} versus B distribution of 266 late-type T = 9, 10 dwarf galaxies with accurate TRGB distance estimates from the UNGC catalog by magnitudes m_{21} and B is shown in the right panel of Fig. 3. As can be seen from these plots, 97% of late-type dwarf galaxies reside in the interval μ = [0.1–10], with a median near $\mu = 1.5$.

Being significantly gas-dominated systems, the late-type dwarf galaxies show the expected correlation between their hydrogen mass and the HI line width W_{50}, which is a baryon analogue of the Tully & Fisher (1977) relation between the integral absolute magnitude of the galaxy, $M_{\rm B}$, and W_{50}. The left panel of Fig. 4 shows the relation between M_{21} and W_{50} for 34 galaxies detected by us. The horizontal bars indicate the standard errors of W_{50}. The dashed line in the panel indicates the relation $M_{\rm B} = -7.27(\log W_{50} - 2.5) - 19.99$ according to Tully et al. (2008) that has been obtained for disc-dominated galaxies. As can be seen from these data, dwarf galaxies satisfactorily follow the classical Tully–Fisher relation when M_{21} magnitudes are used instead of $M_{\rm B}$.

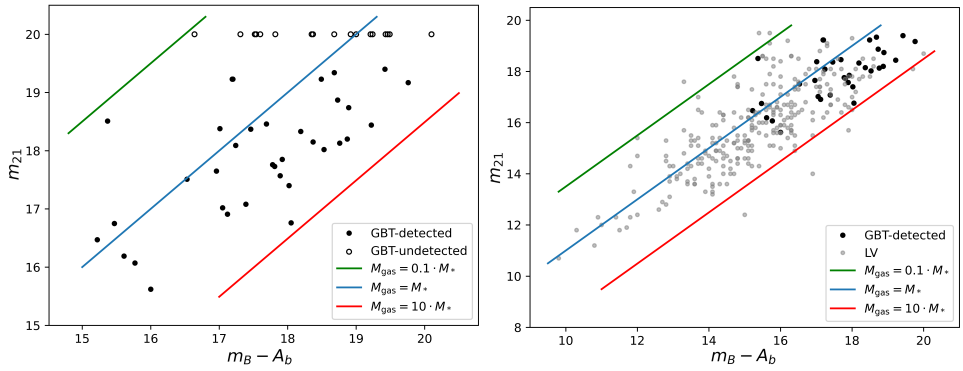

Fig. 3. Distribution of dwarf galaxies by m_{21}-magnitude and B-magnitude corrected for Galactic extinction A_b. Three diagonal lines correspond to μ equal to 0.1, 1 and 10. *Left.* Dwarf galaxies observed with GBT. For undetected galaxies are assigned $m_{21} = 20.^m0$. *Right.* Dwarf galaxies detected with GBT are combined with 266 late-type (T= 9, 10) in the Local Volume with TRGB distance estimates.

The scatter of late-type galaxies in Fig. 4 is not so much caused by measurement errors of W_{50} and S_HI, but by the irregular shape of the dwarfs caused by turbulent motions in them. One would hope that taking the inclination angle of the galaxy into account would reduces the dispersion in the M_{21} vs. W_{50} diagram. The right panel of Fig. 4 exhibits the distribution of irregular dwarfs through M_{21} and corrected for their inclination angle line width W_{50}^c. As one can be seen, taking the tilt into account does not reduce the dispersion of galaxies in the diagram, but actually increases it slightly. The likely reason for the scatter is the real difference in the shape of irregular dwarfs from the ellipsoid of rotation, especially in relation to the shape of their gas component (Roychowdhury et al. 2010).

5 Concluding remarks

The search for new nearby dwarf galaxies using data from the DESI Legacy Imaging Surveys data led to the discovery of more than 50 late-type dwarfs that became targets for observations in the HI line with the GBT. HI fluxes, radial velocities and W_{50} line widths have been measured for 2/3 of the objects. Their median values are 0.53 Jy km/s, 1123 km/s and 33 km/s respectively. According to their D_NAM[3] values, a median distance of 17.3 Mpc and about 40% of the detected galaxies turn out to be new members of the Local Volume with $D < 11$ Mpc. The hydrogen masses are in the range $\log(M_\mathrm{HI}/M_\odot) = [5.68–9.06]$ with a median of 7.68.

[3] D_NAM — kinematic distance of the galaxy in Mpc, calculated via its radial velocity taking into account local streams according to the Numerical Action Method model (Shaya et al. 2017; Kourkchi et al. 2020)

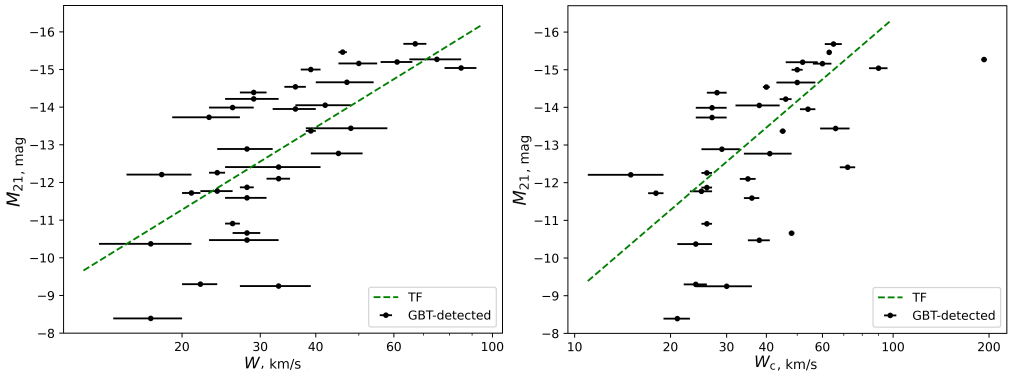

Fig. 4. *Left.* M_{21}-magnitude vs. line width relation for dwarf galaxies detected with the GBT. The horizontal bars show the standard errors of W_{50}. The dashed line displays the Tully–Fisher relation. *Right.* M_{21}-magnitude vs. line width relation for the same galaxies, but with a correction for galaxy inclination.

Our radial velocity measurements led to the discovery of 4 new probable satellites around the LV disc galaxies: NGC 2787, NGC 3556, NGC 4490 and NGC 5055. Also 3 dwarf galaxies: UGC 6451, Dw1235−02 and KDG 162 are close to the bright LV spiral galaxies: M 81, M 104 (Sombrero) and NGC 4605 respectively.

Funding

AN, IK, DM, and MC are supported by the Russian Science Foundation grant № 24–12–00277.

References

Dey A., Schlegel D.J., Lang D., et al., 2019, The Astronomical Journal, 157, p. 168
Karachentsev I.D. and Kaisina E.I., 2022, Astrophysical Bulletin, 77, p. 372
Karachentsev I.D., Karachentseva V.E., Kaisin S.S., et al., 2024, Astrophysics, 66, p. 441
Karachentseva V.E., Karachentsev I.D., Kaisina E.I., et al., 2023, Astronomy & Astrophysics, 678, id. A16
Karachentsev I.D., Makarov D.I., Kaisina E.I., 2013, The Astronomical Journal, 145, p. 101
Kourkchi E., Courtois H.M., Graziani R., et al., 2020, The Astronomical Journal, 159, id. 67
Roychowdhury S., Chengalur J.N., Begum A., et al., 2010, MNRAS, 404, id. L60
Shaya E.J., Tully R.B., Hoffman Y., et al., 2017, The Astrophysical Journal, 850, p. 207
Tully R.B. and Fisher J.R., 1977, Astronomy & Astrophysics, 54, p. 661
Tully R.B., Shaya E.J., Karachentsev I.D., et al., 2008, The Astrophysical Journal, 676, p. 184